Contrasting photoreactivity of β2-adrenoceptor agonists Salbutamol and Terbutaline in the presence of humic substances

Lei Zhou, Mohamad Sleiman, Ludovic Fine, Corinne Ferronato, Pascal de Sainte Claire, Emmanuelle Vulliet, Jean-Marc Chovelon, Guangli Xiu, Claire Richard

Contrasting photoreactivity of β2-adrenoceptor agonists Salbutamol and Terbutaline in the presence of humic substances

Lei Zhou [a,b,c], Mohamad Sleiman [b], Ludovic Fine [d], Corinne Ferronato [d], Pascal de Sainte Claire [b], Emmanuelle Vulliet [e], Jean-Marc Chovelon [d,*], Guangli Xiu [a,c* *], Claire Richard [b,***]

[a] State Environmental Protection Key Lab of Environmental Risk Assessment and control on Chemical Processes. School of Resources & Environmental Engineering, East China University of Science and Technology, Shanghai 200237, China

[b] Université Clermont Auvergne, CNRS, Sigma-Clermont, Institut de Chimie de Clermont-Ferrand, F-63178 Aubière, France

[c] Shanghai Institute of Pollution Control and Ecological Security, Shanghai 200092, PR China

[d] Univ Lyon, Université Claude Bernard Lyon 1, CNRS, IRCELYON, F-69626, 2 Avenue Albert Einstein, Villeurbanne, France

[e] Univ Lyon, CNRS, Université Claude Bernard Lyon 1, ENS de Lyon – Institut des Sciences Analytiques, UMR 5280, 5 rue de la Doua, 69100 Villeurbanne, France

*Corresponding authors.

Email address:

jean-marc.chovelon@ircelyon.univ-lyon1.fr (J-M. Chovelon) ;

xiugl@ecust.edu.cn (G. Xiu);

claire.richard@univ-bpclermont.fr. (C. Richard).

Abstract.

The photodegradation reactions of two typical β2-adrenoceptor agonists, salbutamol (SAL) and terbutaline (TBL), alone, and in the presence of Aldrich humic acid (AHA) or Suwannee River fulvic acid (SRFA) were investigated by steady-state photolysis experiments, laser flash photolysis (LFP), kinetic modeling and quantum calculation. AHA and SRFA (2-20 mgC L^{-1}) accelerated the phototransformation of both SAL and TBL. For SAL, an inhibiting effect of oxygen on the photodegradation was observed that is fully consistent with the main involvement of excited triplet states of HS (^{3}HS*). On the contrary, oxygen drastically enhanced the photodegradation of TBL showing that ^{3}HS* were negligibly involved in the reaction. The involvement of singlet oxygen was also ruled out because of the low reaction rate constant measured between TBL and singlet oxygen. Quantum calculations were therefore performed to explore whether oxygenated radicals could through addition reactions explain the differences of reactivity of TBL and SAL in oxygen medium. Interestingly, calculations showed that in the presence of oxygen, the addition of phenoxyl on TBL led to the formation of adducts and to the loss of TBL while the same addition reaction on SAL partly regenerated the starting compound and at the end degraded SAL less efficiently. This study is of high relevance to understand the processes involved in SAL and TBL phototransformation and the photoreactivity of HS. Moreover, our findings suggest that TBL might be a promising probe molecule to delineate the role of oxygenated radicals.

Keywords: Beta2-adrenoceptor agonists; Photolysis; Humic substances; Oxygenated radicals; Substituted phenols.

1. Introduction

A significant volume of pharmaceuticals are used by humans for the treatment of diseases, injuries, or illnesses, and the occurrence of these chemicals in environment has been widely recognized by scientists, especially in the aquatic environment (Deo, 2014). A wide range of pharmaceuticals are frequently detected in surface, ground and coastal waters with a concentration usually ranging from ng/L to μg/L (Weber et al., 2016; Li, 2014). The continual infusion of pharmaceuticals into surface and drinking waters may lead to chronic exposure to microorganisms and even humans (Crane et al., 2006).

Sunlight-induced direct and indirect photolysis are the primary pathways for abiotic transformation of pharmaceuticals in surface waters (Lee et al., 2014). The direct photolysis of pharmaceuticals results from absorption of solar light by the compound itself, while the indirect photolysis is initiated by light absorption of photo-initiators such as nitrate ions or photosensitizers such as humic substances (HS). HS are brown-colored compounds and show interesting properties under solar irradiation. They can generate reactive species, including triplet excited state (^{3}HS*), hydroxyl radicals (•OH), singlet oxygen ($^1O_2$) and radicals that have all been the subject to an intense research (Zepp et al., 1985; McNeill and Canonica, 2016; Latch and McNeill, 2006; Wang et al., 2007; Blough, 1988; Coelho et al, 2011). The fate of pharmaceuticals in surface waters was shown to be affected by HS (Zhou et al., 2003; Silva et al, 2016; Chen et al., 2017).

Two β_2-adrenoceptor agonists, namely, salbutamol (SAL, also known as albuterol) and terbutaline (TBL) were selected as the target molecules of this study due to their intense uses. SAL is widely used in the treatment of respiratory diseases, such as asthma and chronic obstructive airways disease (Kinali et al., 2002), it has been detected in the surface waters of several European countries with concentrations ranging from 1 to 471 ng L^{-1} (Calamari et al., 2003; Bound and Voulvoulis, 2006; Ternes, 1998). TBL is considered as one of the major

feed additive medicines to increase the proportion of lean meat of livestock (Slotkin and Seidler, 2013). Several studies have been devoted to the phototransformation of SAL and TBL. The quantum yield of photolysis of SAL was measured to be 0.02 for the neutral form and 0.36 for the anionic form upon irradiation between 280 and 380 nm (Dodson et al., 2011; Zhou et al., 2017a). In a study on 27 pharmaceutical molecules SAL and TBL were used along to to establish a correlation between pharmaceuticals photodegradation and the decay of effluent organic matter fluorescence peaks (Yan et al, 2017). SAL and TBL were found to react with the triplet excited states of the effluent organic matter. Another study reported that singlet oxygen contributed highly (19-44%) to the TBL decay when natural organic matter isolates were used to photosensitize the photodegradation of TBL (Yang et al., 2013). Recently, SAL and TBL were found to be both oxidized by sulfate radicals and OH radicals, but interestingly they gave different patterns of reaction. Although the phenoxyl radicals were generated in both cases, SAL finally yielded a benzophenone derivative while TBL gave an adduct by addition of the sulfate radical on the ring (Zhou et al., 2017b).

Here, we compared the phototransformations of SAL and TBL in the presence of two selected HS under solar-light simulated irradiation. A special attention was given to the nature of reactive species involved, and to the photoproducts characterization. This study revealed that oxygen affected the two molecules phototransformation very differently and quantum calculations were performed to better understand the differences in the reactivity. The results obtained from this study would be helpful in predicting the photochemical fate of β_2-adrenoceptor agonists, as well as the impact of HS on similar emerging contaminants.

2. Material and methods

2.1 Chemicals.

Salbutamol hemisulfate (SAL, 98%), terbutaline hemisulfate (TBL, 98%), formic acid (FA, 96%), furfuryl alcohol (FFA, 98%), *p*-nitroanisole (PNA, 97%), pyridine (PYR, 96.5%) and sorbic acid (SA, 98%) were purchased from Sigma-Aldrich. 3-Carboxybenzophenone (99%) was purchased from ACROS and Suwannee River fulvic acid (SRFA, 1R101F) of reference grade was obtained from the International Humic Substances Society (IHSS). Humic acid (AHA) was provided by Sigma-Aldrich. HPLC or LC-MS grade acetonitrile (ACN), methanol (MeOH), and 2-propanol were supplied by Fisher Chemical. Other reagents were at least of analytical grade and used as received without further purification. Milli-Q water (18.2 MΩ cm) was prepared from a Millipore Milli-Q system. Oxygen and helium used for oxygenation and deoxygenation were of ultrapure quality (Air Products).

2.2 Photochemical Experiments.

Steady-state irradiation experiments were conducted in a home-made photochemical reactor equipped with a 125 W high pressure mercury lamp (Cathodeon, Cambridge, UK) housed in a borosilicate immersion wall ($\lambda > 290$ nm) (Figure SM-1, Supplementary Material). The lamp was turned on for 20 min prior to irradiations for warming, then, 50 mL of solutions were poured in a Pyrex-glass reactor (i.d. = 5 cm, height = 15 cm) and irradiated for different times. The reactor placed in the photo-reactor was maintained at 24 ± 1 °C using a cooling water circulation system. Typically, the solutions were maintained in contact with air. Some experiments were also conducted on over-oxygenated or deoxygenated solutions. For this, we bubbled a stream of O_2 in the first case, and a stream of helium in the second case during the whole irradiations. The pH of the starting solutions was adjusted to 8 using phosphate buffers. 2-propanol (10 mM) was used as an OH radical scavenger to measure the involvement of $OH^{\cdot}$ radicals. Furfuryl alcohol (60 μM) was used as a $^1O_2$ probe and sorbic acid (SA, 100 μM) as a triplet scavenger to confirm the involvement of $^3HS^*$. Aliquots of 1 mL of the irradiated

122 solutions were withdrawn at predetermined times and analyzed directly by HPLC. The
123 detailed analytical methods are described in the Supplementary Material (Text SM-1).
124 **2.3 Laser flash photolysis experiments.** Laser flash photolysis (LFP) experiments were
125 carried out using a Quanta Ray GCR 130 Nd: YAG laser and an Applied Photophysics station
126 previously described (Bonnichon et al., 1998). The aqueous solutions were irradiated at 266
127 nm using the fourth harmonic of the laser. 3-carboxybenzophenone (CBP) was selected as a
128 model sensitizer of HS. The rate constants of reactions of SAL and TBL with ^{3}CBP* were
129 measured by monitoring the decay of ^{3}CBP* at 520 nm. A red filter was placed between the
130 cell and the photomultiplicator to avoid parasitic signals. SAL and TBL were added in the
131 concentration range (0-400 μM).
132 **2.4 Quantum calculations.** The Gaussian09 series of programs (Frisch et al., 2010) was used
133 to perform Density Functional Theory (DFT) calculations at the B3LYP/6–31+G(d,p) level.
134 The Polarizable Continuum Model (PCM) (Tomasi et al., 2005) was used throughout to
135 model the solvent (water) implicitly. Calculations were performed to obtain Transition States,
136 minimum energy structures, Intrinsic Reaction Coordinate (IRC) paths and Minimum Energy
137 Pathways (MEP). An extensive search for conformers was pursued first in order to locate the
138 global minimum energy species (geometry given in SI section). This was achieved by a
139 systematic investigation of the variations of the Potential Energy Surface (PES) along key
140 dihedral angles.
141
142 **3. Results and discussion**
143 **3.1 Direct photodegradation**
144 In air-saturated medium and at pH 8.0, both substrates underwent photolysis. Pseudo-
145 first-order kinetics fitted the photodegradation curves of SAL and TBL until conversion
146 extents of 50 % (Eq 1):

147 $$\ln([P]_t/[P]_0) = -k_{obs}t \quad (1)$$

148 where P represents the target compound (SAL or TBL), and k_{obs} (s^{-1}) the apparent first-order
149 degradation rate constant. TBL (60 μM) was photodegraded faster ($k_{obs} = (6.9 \pm 0.2) \times 10^{-5}$ s^{-1})
150 than SAL ($k_{obs} = (3.0 \pm 0.1) \times 10^{-5}$ s^{-1}) (Figure 1). The photodegradations occurred due to the
151 overlapping of the absorption spectra of TBL and SAL with the emission spectrum of the
152 HPK lamp filtered by the Pyrex glass reactor (> 290 nm). Laser flash photolysis experiments
153 confirmed the photoionization processes and the formation of phenoxyl radicals ($SAL_{-H}^{\bullet}$ or
154 $TBL_{-H}^{\bullet}$) (Zhou et al., 2017b).
155
156 **3.2 Accelerating effect of HS in air-saturated medium**
157 Then, SRFA and AHA were added to SAL and TBL solutions at concentrations
158 comprised between 2 and 20 mgC L^{-1}. Figure 1 reveals that the photodegradations of SAL and
159 TBL in air-saturated solution were significantly enhanced by the addition of SRFA or AHA.
160 Moreover, increasing the HS concentrations led to an increase of k_{obs} values. The
161 enhancement was more pronounced for TBL than for SAL. For instance, in the presence of 20
162 mgC L^{-1} of AHA, the degradation rate constant of TBL was 3.8-fold higher compared to that
163 of the control sample (k_{obs} equal to 38×10^{-5} s^{-1} against 7.0×10^{-5} s^{-1} without AHA), while in the
164 case of SAL, k_{obs} was only 1.9 fold higher (5.8×10^{-5} s^{-1} against 3.0×10^{-5} s^{-1} for the control
165 sample without AHA).
166 **Figure 1**
167
168 **3.3 Photoproducts.**
169 We investigated the effect of AHA and SRFA on the SAL and TBL photoproducts. In
170 general, the same photoproducts were detected in the absence and in the presence of 10 mgC
171 L^{-1} of HS (details in Table SM-2 and SM-3, SM). In the case of SAL, we identified by HPLC-

MS analysis 2-(*tert*-butylamino)-1-(4-hydroxyl-3-hydroxymethylphenyl) ethanone (SAL_{-2H}), 2-(*tert*-butylamino)-1-(4-hydroxyl-3-hydroxymethylphenyl) ethylene (SAL_{-H2O}) and the hydroxylated product of SAL_{-2H} (SAL_{-2H+O}) as the main photoproducts (Figure 2). For TBL, 2-(*tert*-butylamino)-1-(2,3,5-trihydroxylphenyl) ethanol (TBL_{-H+OH}) and 5-[2-(tert-butylamino)-1-hydroxyethyl]-2-hydroxyl-1,4-benzoquinone (TBL_{+O-2H}) were found (Figure 2). Some of these photoproducts were reported in the literature, in particular the hydroxybenzoquinone derivative of TBL (TBL_{+O-2H}) (Yang et al, 2013; Yan et al, 2017). However, from the quantitative point of view, we got some differences. After a conversion extent of 10%, the area of the SAL photoproduct detected in HPLC-UV was of 1100 ± 50 at 224 nm, both in the absence as in the presence of AHA, while the area of the TBL photoproduct showed a peak area of 2500 ± 53 at 230 nm in the absence of AHA, but of only 700 ± 20 in the presence of AHA. These results suggest that a significant change of reaction occurred for TBL but not for SAL.

Figure 2

3.4 Reactivity of SAL and TBL toward singlet oxygen and ^{3}CBP*.

When irradiated in the presence of HS, SAL and TBL might react with $^1O_2$ and ^{3}HS*. To further evaluate the contribution of these species in the HS-mediated photoreactions, we first measured their reactivities with our substrates. The reaction rate constants of SAL and TBL with $^1O_2$ were obtained using Rose Bengal as a sensitizer, and FFA as a reference compound, as described in Text SM-2 of SM. The reactivities of SAL and TBL with ^{3}HS* were estimated using CBP as a proxy HS sensitizer (Avetta et al, 2016).

In the case of TBL, a rate constant of $(8.0 \pm 0.3) \times 10^6$ $M^{-1}s^{-1}$ at pH 8.0 was determined for the reaction with $^1O_2$. This is comparable to the value of $(7.1 \pm 0.3) \times 10^6$ $M^{-1}s^{-1}$ reported in the literature at pH 7.0 by Yang et al., 2013. For SAL a reaction rate constant of (1.1 ± 0.1)

197 $\times 10^8$ $M^{-1}s^{-1}$, i.e. ~14 fold faster than that of TBL was determined. The reaction rate constants
198 of ^{3}CBP* with TBL and SAL were directly measured by laser flash photolysis. We got (2.7 ±
199 0.3) × 10^9 $M^{-1}s^{-1}$ and (6.0 ± 0.6) × 10^9 $M^{-1}s^{-1}$, respectively.
200
201 **3.5 Reactive species involved in the HS-mediated photoreactions**.
202 In this section, we investigated the effect of AHA and SRFA (5 mgC L^{-1}) on the rate
203 of SAL and TBL photodegradation. In these conditions, k_{obs} is the sum of 2 terms, one
204 corresponding to the direct photolysis and the other to the sensitized or indirect reaction. At
205 the level of 5 mgC L^{-1} AHA and SRFA reduced the absorbances of SAL and TBL by 60%
206 and 35%, respectively, through screen effect filter (Table SM-4, SM). Therefore, the direct
207 photodegradation rate constants of SAL and TBL (k_{direct}) have to be corrected for this screen
208 effect. The corrected k_{direct} are finally equal to 1.2×10^{-5} s^{-1} and 2.0×10^{-5} s^{-1} for SAL in the
209 presence of AHA and SRFA and to 2.6×10^{-5} s^{-1} and 4.2×10^{-5} s^{-1} for TBL in the presence of
210 AHA and SRFA (Table 1). Hereinafter, the indirect degradation rate constants $k_{indirect}$ will be
211 calculated according to:
212 $$k_{indirect} = k_{obs} - \text{corrected } k_{direct} \quad (2)$$
213 *i) Hydroxyl radical.* In order to test the involvement of $HO^{\cdot}$, 10 mM of 2-propanol, used as a
214 $HO^{\cdot}$ scavenger ($k = 1.9 \times 10^9$ M^{-1} s^{-1}), were spiked into the reaction solutions. The addition of
215 2-propanol in excess had no effect on the SAL photodegradation rate and decreased that of
216 TBL by less than 10% (Figure SM-2, SM). Thus, the involvement of $HO^{\cdot}$ in the reactions was
217 very limited despite the high reactivity of SAL and TBL with OH ($k_{\cdot OH, SAL} = (5.3 \pm 0.7) \times 10^9$
218 M^{-1} s^{-1} and $k_{\cdot OH, TBL} = (5.9 \pm 0.8) \times 10^9$ M^{-1} s^{-1}) (Zhou et al., 2017b).
219 ii) *Humic triplet state.* To investigate the contribution of ^{3}HS* in the HS-mediated
220 photodegradations, experiments were conducted at different oxygen concentrations because
221 oxygen is a well-known triplet scavenger. Removal of oxygen by continuous helium (He)

purging should led to an increase of the steady-state concentration of $^3HS^*$, $[^3HS^*]ss$ and thus to an increase of $k_{indirect}$ if $^3HS^*$ is involved in the reactions. As seen in Figure 3, the rate of SAL phototransformation in the presence of AHA and SRFA was much higher in helium-purged solution than that in air-saturated medium. The indirect rate constants were in the range (17-18) $\times 10^{-5}$ s^{-1} in He-saturated medium against (2.8-3.1) $\times 10^{-5}$ s^{-1} in air-saturated medium (Table 1). This result demonstrates the involvement of $^3HS^*$ in the reactions. The involvement of $^3HS^*$ was confirmed by adding the triplet quencher, sorbic acid (SA, 100 μM) in the presence of which the SAL indirect photodegradation rate constant was reduced by a factor of 2 in air-saturated solution. In contrast, for TBL, the solution deoxygenation through He purging reduced the indirect rate to (3.2-3.3) $\times 10^{-5}$ s^{-1} against (12.1-18.9) $\times 10^{-5}$ s^{-1} (Table 1). This result is opposite to the one found for SAL. Afterwards, the addition of SA (100 μM) did not show a significant effect on k_{obs}, confirming that $^3HS^*$ contributed in a minor way to the TBL photodegradation.

At last, the solutions of SAL and TBL containing SRFA or AHA were irradiated after having been saturated by oxygen. For SAL, $k_{indirect}$ became very low (0.2-0.8) $\times 10^{-5}$ s^{-1} while in the case of TBL, $k_{indirect}$ was close to the one measured in air-saturated medium (Figure 3 and Table 1).

Figure 3

To rationalize these results, mechanistic analysis is necessary. In a simplified mechanism, we considered that $^3HS^*$ produced in (3) undergoes desactivation (4), oxidizes SAL and TBL, labeled as P, by electron transfer or H atom abstraction (5), or reacts with oxygen to yield $^1O_2$ (6). We make the hypothesis that the yield of $^1O_2$ formation in process (6) is equal to 1:

$$HS + h\nu \rightarrow {}^1HS^* \rightarrow {}^3HS^* \qquad (3)$$

$$^3HS^* \rightarrow HS \qquad (4)$$

$$^3HS^* + P \rightarrow HS^{\bullet-} + H^+ + P\text{-}H^{\bullet} \quad (5)$$

$$^3HS^* + O_2 \rightarrow HS + {}^1O_2 \quad (6)$$

$$P + {}^1O_2 \rightarrow \text{products} \quad (7)$$

$$^1O_2 \rightarrow O_2 \quad (8)$$

Photoproducts of P are expected to arise from further reactions of $P\text{-}H^{\cdot}$ and from reaction (7). The lowest triplet (E_{T1}) excitation energy of SAL was calculated as 3.68 eV in our previous work (Zhou et al., 2017a), which is larger than that of most kinds of HS (2.23 – 2.60 eV, for SRFA, E_{T1} was 2.37 eV) (Zhang et al., 2010). Thus, energy transfer from $^3HS^*$ to SAL is not possible from a thermodynamical point of view, and we excluded this reaction in the proposed mechanism.

In He-saturated solution, the rate of HS-mediated phototransformation of P is equal to:

$$r^{He}_{indirect} = k_5[^3HS^*]_{SS}[P] \quad (9)$$

where $[^3HS^*]_{SS}$ the steady-state concentrations of $^3HS^*$ is equal to:

$$[^3HS^*]_{SS} = I_a^{HS} \Phi_T^{HS} / (k_4 + k_5[P]) \quad (10)$$

with I_a^{HS} represents the rate of photon absorption by HS and Φ_T^{HS} is the quantum yield of $^3HS^*$ generation.

In air-saturated solution, the rate of indirect P phototransformation can be written as :

$$r^{Air}_{indirect} = k_5[^3HS^*]_{SS}[P] + k_7[^1O_2]_{SS}[P] \quad (11)$$

with

$$[^3HS^*]_{SS} = \frac{I_a^{HS}\Phi_T^{HS}}{k_4 + k_6[O_2] + k_5[P]} \quad (12)$$

As the rate constants of reaction with $^1O_2$ are respectively 55 and 32-fold lower than the rate constants of reaction with ^{3}CBP* for SAL and TBL, Eq 11 can be simplified, in a first approximation, by neglecting the term corresponding to $^1O_2$. This gives:

$$r^{P,\,He}_{indirect} / r^{P,\,Air}_{indirect} = (k_4 + k_6[O_2] + k_5[P]) / (k_4 + k_5[P]) \qquad (13)$$

If the scheme and assumptions are correct, the experimental ratios must be higher than 1. It is the case for SAL with 6.3 in the case of SRFA and 5.8 in the case of AHA. Taking $k_4 \approx 5\times10^4\ s^{-1}$ (Huber et al., 2003), $k_6[O_2] \approx 5\times10^5\ s^{-1}$ (data provided by Canonica et al., 1995 in the case of natural waters), we finally get $k_5 \approx 10^9\ M^{-1}\ s^{-1}$. This value is consistent with data obtained with other electron-rich phenols (McNeill and Canonica, 2016; Canonica et al., 1995), but it is 6-fold lower than that measured using 3-carboxybenzophenone as a sensitizer.

For TBL however, the ratio is much less than 1 (0.26 and 0.17 for SRFA and AHA, respectively) showing that assumptions/scheme are not working in this particular case. In air-saturated solution, the percentage of ^{3}HS* trapped by oxygen is equal to $100\times k_6[O_2]/(k_6[O_2] + k_4 + k_5[P])$ and thus to 80%. On the other hand, the percentage of $^1O_2$ trapped by TBL is equal to $100\times k_7[TBL]/(k_7[TBL] + k_8[H_2O])$. Given the value of $k_7 = (8.0 \pm 0.3)\times10^6\ M^{-1}s^{-1}$, and $k_8 \approx 2.3\times10^5\ s^{-1}$ in water (Rodgers and Snowden, 1982), TBL at the concentration of 60 µM only trapped 0.2% of $^1O_2$. If we assume that SAL trapped all the ^{3}HS* in the absence of oxygen, it gives a rate of ^{3}HS* formation of $1.1\times10^{-8}\ M\ s^{-1}$ and a rate of formation of $^1O_2$ of $0.88\times10^{-8}\ M\ s^{-1}$ in air-saturated medium. The percentage of $^1O_2$ trapped by TBL being of 0.2%, the rate of reaction of TBL with $^1O_2$ was equal to $1.8\times10^{-11}\ M\ s^{-1}$ fully negligible behind the rate of TBL decay $1.1\times10^{-8}\ M\ s^{-1}$ for AHA and $7.2\times10^{-9}\ M\ s^{-1}$ for SRFA, ruling out a significant importance of this pathway in the HS-mediated phototransformation.

293 The low rate of TBL photodegradation in the absence of oxygen is not consistent
294 with the high reactivity of TBL with ^{3}HS* deduced from the high rate constant measured
295 between ^{3}CBP* and TBL. The explanation of this apparent discrepancy could be that TBL
296 is actually oxidized by ^{3}HS* at a significant rate (process 5) but regenerated through
297 process (5'). Such reactions have been shown to take place (Vione et al, 2018).

298 $$HS + P\text{-}H^{\bullet} \rightarrow HS\text{-}H^{\bullet} + P \qquad (5')$$

299 If reaction (5') also occurs for SAL, the rate constant k_5 deduced from Eq 13 may be
300 minimized. This is in accordance with the low value of calculated k_5 from Eq 13 compared to
301 that obtained in the experiment with ^{3}CBP*.

302 The possible existence of reaction 5' does not explain however why in air and oxygen
303 saturated media the photodegradation of TBL was so fast. Apart commonly mentioned
304 reactive species, radicals that are surely formed in significant amounts in irradiated HS
305 solutions (Blough, 1988) might be responsible for these our results and this option needs to be
306 explored. Due to the difficult to generate oxy and peroxy radicals in water by selective
307 excitation, we performed quantum calculations to determine in which conditions and for
308 which reasons oxygenated radicals in the presence of oxygen would induce degradation of
309 TBL but not of SAL.

310

311 **3.6 Reactivity of TBL and SAL with phenoxyl radicals**

312 These calculations were performed using the phenoxyl radical as reacting radical
313 because phenols are a class of oxygenated radicals well represented in humic materials.
314 Moreover, humic substances produces long-lived phenoxyl radicals (Golanoski et al, 2012;
315 Chen et al, 2018). In these calculations, we first investigated the reactivity of TBL and SAL
316 with $^3O_2$ and phenoxyl radicals Two different pathways were investigated: one where $^3O_2$ or

PhO reacted first in H radical abstraction reactions, the other where PhO reacted through an addition reaction on TBL, followed by oxygen addition (see Scheme 1).

Both reactions are endothermic overall, but the reaction energy is significantly more favorable in reaction 1b. A reaction energy of +31.2 kcal/mol was found for 1a when reactive species was PhO (+61.2 kcal/mol for $^3O_2$). In comparison, the reaction energy was +18.3 kcal/mol for the phenoxyl radical addition, and +12.0 overall for 1b. Thus, reaction 1b, being thermodynamically more favorable, was investigated more thoroughly. A transition state (see SM) was found for the addition reaction of PhO. Secondly, the addition reaction of $^3O_2$ was barrierless. It was also found that the potential energy surfaces did not exhibit significant differences between TBL and SAL (activation energies were respectively 21.9 and 22.8 kca/mol; see Figure 4). Thus, it was decided to investigate the fate of peroxyl radical **I** for TBL and SAL in order to understand the differences of reactivities that were observed experimentally.

The peroxyl radical **I** in Figure 4 can abstract a hydrogen atom on the cycle (H_a in Figure 4) or on the chain (H_b). For TBL, both pathways require similarly activation energies. Abstraction of H_b requires lower energy and is slightly more favorable (activation energy is 36.8 kcal/mol, while it is 37.7 kcal/mol for H_a). MEP calculations were performed to obtain the PES for HO_2 dissociation from species **II** (see Figure 5). This was achieved by computing partial optimizations for fixed C-OOH bond lengths. It was found that 2.2 kcal/mol was required to dissociate HO_2 from **II**. Further keto-enol rearrangement gives the more stable degradation product **III** (see Figure 5). Note that abstraction of H_a or H_b leads indistinctly to the same degradation product **III**.

Similarly, for SAL, H_a abstraction was slightly less favorable than that of H_b (activation energy is 36.7 kcal/mol whereas it was 32.9 kcal/mol for H_b). However, for TBL the position of the hydroperoxyl group in **II** (adjacent to the radical site) leads readily to a

342 stable closed-shell species, for SAL, the positions of the hydroperoxyl and the radical site in
343 **II** are in meta position and the closed-shell species cannot be reached easily. Spin density in II
344 is larger on the ring (0.70) that on the chain (0.45; see SM). In that case, dissociation of HO_2
345 (obtained from MEP calculations) lead to the spontaneous dissociation of radical PhO, a
346 reaction that yields the reactant species.

347 Finally, the experimental photodegradation rate constants ($1\text{-}20\times10^{-5}$ s^{-1}) found in this
348 work were coherent with the activation energies found from our theoretical calculations. For
349 example, unimolecular rate constants that range between 10^{-5} s^{-1} and 20×10^{-5} s^{-1} require
350 activation energies of 24.3 and 22.5 kcal/mol, respectively (see Eq 14). The activation
351 energies calculated for the limitant unimolecular reactions depicted in Figure 5 have
352 activation energies of 24.8 and 20.5 kcal/mol, in agreement with the experimental results.

353 $$k_{uni} = \frac{k_B T}{h} e^{-\Delta G / k_B T} \qquad (14)$$

354 Moreover, if one considers the bimolecular association reaction of PhO and TBL (or
355 SAL) in Figure 4 to be the limitant step, and provided the concentration of PhO is ~10^{-6} M, an
356 activation energy between 16.2 and 18.0 kcal/mol is required to obtain apparent first order
357 rate constants of 20×10^{-5} s^{-1} and 10^{-5} s^{-1}, respectively (See Eq 15). This is slightly smaller than
358 the values found in this work (21.9 ad 22.8 kcal/mol for TBL and SAL, respectively).
359 However, the overall concentration of alkoxy radicals in HS is not well known and may be
360 larger than 10^{-6} M. In conclusion, our experimental data show that the limiting step in the
361 degradation process requires an activation energy of ~20 kcal/mol, which is in agreement with
362 our theoretical results. Note also that the energies calculated in our work are obtained for a
363 standard state of 1 atm, and it was necessary to multiply our rate constant by 0.08206T in
364 order to have the proper reference standard state, i.e. 1 mol/L (de Sainte Claire et al., 1996;
365 Bryantsev et al, 2008).

366 $$k_{apparent\ uni} = [\mathrm{PhO}] \times 0.08206T \times \frac{k_B T}{h} e^{-\Delta G / k_B T} \quad (15)$$

367 Thus, the different reactivities observed experimentally between TBL and SAL may be
368 explained mainly by the differences of the positions of the alcohol groups on the phenyl
369 ring. For SAL, the photodegradation rate constant is smaller because the reaction with
370 oxygen yields the reactant back.

371

372 **4. Conclusion**

373 To conclude, the present study focused on the photo-transformation of two β2-
374 adrenoceptor agonists. In pure water the direct photolyses were relatively slow, but the
375 presence of HS significantly enhanced reactions. Therefore, β2-adrenoceptor agonists are
376 expected to be photolyzed in surface waters enriched in natural organic matter and terrestrial
377 inputs. Although SAL and TBL share common side chain, their major photooxidation
378 pathways in the presence of HS were very different. For SAL, the enhancement by HS was
379 essentially due to ^{3}HS*and $^1O_2$. In the case of TBL that underwent faster photodegradation in
380 air-saturated medium than SAL, none of these species was significantly involved. Quantum
381 calculations suggest that oxygenated such as phenoxyl radicals could sgnificantly enhance the
382 photodegradation of TBL through addition reactions. This study and in particular the
383 unexpected behavior of TBL stresses several points. First, the different behaviors of SAL and
384 TBL in HS remind us that different substituted phenols would undergo different
385 photochemical fates in natural waters. Second, the influence of quenchers like HS should be
386 considered carefully and comprehensively, depending on the target substances. Third, TBL
387 could be a potential probe molecule for oxygenated radicals.

388

389 **Acknowledgement**

This work was supported by the National Natural Science Foundation of China (No. 21806037). Lei Zhou would like to acknowledge the support from the China Scholarship Council (CSC, 201406190169).

References

Avetta, P., Fabbri, D., Minella, M., Brigante, M., Maurino, V., Minero, C., Pazzi, M., Vione, D., 2016. Assessing the phototransformation of diclofenac, clofibric acid and naproxen in surface waters: Model predictions and comparison with field data. Water Res. 105, 383-394.

Blough, N. V., 1988. Electron paramagnetic resonance measurements of photochemical radical production in humic substances. 1. Effects of oxygen and charge on radical scavenging by nitroxides. Environ Sci Technol 22, (1), 77-82.

Bonnichon, F., Richard, C., 1998. Phototransformation of 3-hydroxybenzonitrile. J. Photochem. Photobiol. A 119, 25-32.

Bound, J. P., Voulvoulis, N., 2006. Predicted and measured concentrations for selected pharmaceuticals in UK rivers: Implications for risk assessment. Water Res 40, (15), 2885-2892.

Bryantsev, V. S., Diallo, M. S., Goddard III, W. A., 2008. Calculation of solvation free energies of charged solutes using mixed cluster/continuum models. J. Phys. Chem. B 112, 9709-9719.

414 Calamari, D., Zuccato, E., Castiglioni, S., Bagnati, R., Fanelli, R., 2003. Strategic survey of
415 therapeutic drugs in the rivers Po and Lambro in northern Italy. Environ Sci Technol 37, (7),
416 1241-1248.
417
418 Chen Y., Liu L., Liang J., Wu B., Zuo J., Zuo Y., 2017. Role of humic substances in the
419 photodegradation of naproxen under simulated sunlight. Chemosphere 187, 261-267.
420
421 Chen, Y., Zhang, X., Feng, S., 2018. Contribution of the Excited Triplet State of Humic Acid
422 and Superoxide Radical Anion to Generation and Elimination of Phenoxyl Radical. Environ.
423 Sci. Technol. 52, 8283-8291.
424
425 Coelho C.; Guyot G.; ter Halle A.; Cavani L.; Ciavatta C.; Richard C., 2011. Photoreactivity
426 of humic substances: relationship between fluorescence and singlet oxygen production
427 Environ. Chem. Let 9, 447-451.
428
429 Crane, M.; Watts, C.; Boucard, T., 2006. Chronic aquatic environmental risks from exposure
430 to human pharmaceuticals. Sci Total Environ 367, (1), 23-41.
431
432 Deo, R. P., 2014. Pharmaceuticals in the surface water of the USA: A review. Curr Environ
433 Health Rep. 1(2), 113-122.
434
435 Dodson, L. G., Vogt, R. A., Marks, J., Reichardt, C., Crespo-Hernandez, C. E. 2011.
436 Photophysical and photochemical properties of the pharmaceutical compound salbutamol in
437 aqueous solutions Chemosphere 83(11), 1513-1523.
438

Frisch, M.J., Trucks, G.W., Schlegel, H.B., Scuseria, G.E., Robb, M.A., Cheeseman, J.R., Scalmani, G., Barone, V., Mennucci, B., Petersson, G.A., Nakatsuji, H., Caricato, M., Li, X., Hratchian, H.P., Izmaylov, A.F., Bloino, J., Zheng, G., Sonnenberg, J.L., Hada, M., Ehara, M., Toyota, K., Fukuda, R., Hasegawa, J., Ishida, M., Nakajima, T., Honda, Y., Kitao, O., Nakai, H., Vreven, T., Montgomery Jr., J.A., Peralta, J.E., Ogliaro, F., Bearpark, M., Heyd, J.J., Brothers, E., Kudin, K.N., Staroverov, V.N., Keith, T., Kobayashi, R., Normand, J., Raghavachari, K., Rendell, A., Burant, J.C., Iyengar, S.S., Tomasi, J., Cossi, M., Rega, N., Millam, J.M., Klene, M., Knox, J.E., Cross, J.B., Bakken, V., Adamo, C., Jaramillo, J., Gomperts, R., Stratmann, R.E., Yazyev, O., Austin, A.J., Cammi, R., Pomelli, C., Ochterski, J.W., Martin, R.L., Morokuma, K., Zakrzewski, V.G., Voth, G.A., Salvador, P., Dannenberg, J.J., Dapprich, S., Daniels, A.D., Farkas, O., Foresman, J.B., Ortiz, J.V., Cioslowski, J., Fox, D.J., 2010. Gaussian09, Revision C.01, Gaussian, Inc, Wallingford CT.

Golanoski, K. S., Fang, S., Del Vecchio, R., Blough, N. V., 2012. Investigating the mechanism of phenol photooxidation by humic substances. Environ Sci Technol 46, (7), 3912-3920.

Grebel, J. E., Pignatello, J. J., Mitch, W. A., 2011. Sorbic acid as a quantitative probe for the formation, scavenging and steady-state concentrations of the triplet-excited state of organic compounds. Water Res. 45, (19), 6535-6544.

Huber, M. M.; Canonica, S.; Park, G.-Y.; Von Gunten, U., 2003. Oxidation of pharmaceuticals during ozonation and advanced oxidation processes. Environ Sci Technol. 37, (5), 1016-1024.

Kinali, M., Mercuri, E., Main, M., De Biasia, F., Karatza, A., Higgins, R., Banks, L., Manzur, A.; Muntoni, F., 2002. Pilot trial of albuterol in spinal muscular atrophy. Neurology 59, (4), 609-610.

Latch, D. E.; McNeill, K., 2006. Microheterogeneity of singlet oxygen distributions in irradiated humic acid solutions. Science. 311, (5768), 1743-1747.

Lee, E., Shon, H. K., Cho, J., 2014. Role of wetland organic matters as photosensitizer for degradation of micropollutants and metabolites. J. Hazard. Mat 276, 1-9.

Li, W. C., 2014. Occurrence, sources, and fate of pharmaceuticals in aquatic environment and soil. Environ Pollut 187, 193-201.

McNeill, K., Canonica, S., 2016. Triplet state dissolved organic matter in aquatic photochemistry: reaction mechanisms, substrate scope, and photophysical properties. Environ. Sci.: Processes & Impacts 18, (11), 1381-1399.

Rodgers, M. A.; Snowden, P. T., 1982. Lifetime of oxygen (O2 (1. DELTA. g)) in liquid water as determined by time-resolved infrared luminescence measurements. J. Am. Chem. Soc. 104, (20), 5541-5543.

de Sainte Claire, P., Song, K., Hase, W. L., Brenner, D. W., 1996. Comparison of ab initio and empirical potentials for H-atom association with diamond surfaces. J. Phys. Chem. 100, 1761-1766.

489 Silva C. P., Lima D. L. D., Groth M. B., Otero M., Esteres V. I. 2016. Effect of natural
490 aquatic humic substances on the photodegradation of estrone, 2016. Chemosphere 145, 249-
491 255.
492
493 Slotkin, T. A., Seidler, F. J., 2013. Terbutaline impairs the development of peripheral
494 noradrenergic projections: Potential implications for autism spectrum disorders and
495 pharmacotherapy of preterm labor. Neurotoxicol Teratol 36, 91-96.
496
497 Ternes, T. A., Occurrence of drugs in German sewage treatment plants and rivers, 1998.
498 Water Res 32, (11), 3245-3260.
499
500 Tomasi, J., Mennucci, B., Cammi, R., 2005. Quantum Mechanical Continuum Solvation
501 Models. Chem. Rev. 105, 2999–3094.
502
503 Vione, D.; Fabbri, D.; Minella, M.; Canonica, Silvio, 2018. Effects of the antioxidant
504 moieties of dissolved organic matter on triplet-sensitized phototransformation processes:
505 Implications for the photochemical modeling of sulfadiazine.Water Res. 128, 38-48.
506
507 Wang, W., Zafiriou, O. C., Chan, I.-Y., Zepp, R. G., Blough, N. V., 2007. Production of
508 hydrated electrons from photoionization of dissolved organic matter in natural waters.
509 Environ Sci Technol 41, (5), 1601-1607.
510
511 Weber, F. A., Bergmann, A., Hickmann, S., Ebert, I., Hein, A., Küster, A., 2016.
512 Pharmaceuticals in the environment-Global occurrences and perspectives. Environ Toxicol
513 Chem 35, (4), 823-835.

514

515 Yan, S., Yao, B., Lian, L., Lu, X., Snyder, S.A., Li, R., Song, W. 2017. Development of
516 fluorescent surrogates to predict the photochemical transformation of pharmaceuticals in
517 wastewater effluents. Environ. Sci. Technol. 51 (5), 2738-2747.

518

519 Yang, W., Abdelmelek, S. B., Zheng, Z., An, T., 2013. Zhang, D.; Song, W., Photochemical
520 transformation of terbutaline (pharmaceutical) in simulated natural waters: Degradation
521 kinetics and mechanisms. Water Res 47, (17), 6558-6565.

522

523 Zepp, R. G., Schlotzhauer, P. F., Sink, R. M., 1985. Photosensitized transformations
524 involving electronic energy transfer in natural waters: role of humic substances. Environ. Sci.
525 Technol.19, (1), 74-81.

526

527 Zhang, S., Chen, J., Qiao, X., Ge, L., Cai, X., Na, G., 2010. Quantum chemical investigation
528 and experimental verification on the aquatic photochemistry of the sunscreen 2-
529 phenylbenzimidazole-5-sulfonic acid. Environ Sci Technol 44, (19), 7484-7490.

530

531 Zhou, L.; Wang, Q.; Zhang, Y; Ji, Y; Yang, X, 2017a. Aquatic photolysis of β2-agonist
532 salbutamol: kinetics and mechanism studies. Environ. Sci. Poll. Res. 24(6), 5544-5553.

533

534 Zhou, L., Sleiman, M., Ferronato, C., Chovelon, J.-M., de Sainte-Claire, P., Richard, C.,
535 2017b. Sulfate radical induced degradation of β2-adrenoceptor agonists salbutamol and
536 terbutaline: Phenoxyl radical dependent mechanisms. Water Res. 123, 715-723.

537

538 Zhou C., Chen J., Xie Q., Wei X., Zhang Y., Fu Z., 2015. Photolysis of three antiviral drugs
539 acyclovir, zidovudine and lamivudine in surface freshwater and seawater. Chemosphere 138,
540 792-797.
541
542
543

544 CAPTIONS FOR FIGURES

545

546 Figure 1. Photodegradation rate constants of SAL (60 μM) and TBL (60 μM), k_{obs}, in the
547 presence of different concentrations of Suwannee River Fulvic Acid Standard II (SRFA) and
548 Aldrich Humic Acid (AHA) under HPK irradiation, at pH = 8.0 and in air-saturated medium.
549 Error bars represent the standard deviation.

550

551 Figure 2. Photoproducts of SAL and TBL as identified by HPLC/MS.

552

553 Figure 3. Photodegradation rate constants of SAL and TBL (60 μM), k_{obs}, under different
554 conditions in the presence of 5 mg C L^{-1} HS under HPK irradiation, pH = 8.0, $[SA]_0$ = 100
555 μM. Error bars represent the standard deviation.

556

557 Figure 4: The consecutive addition reactions of PhO and $^3O_2$ on TBL. Electronic energies
558 (kcal/mol) were obtained at the B3LYP/6-31+G(d,p)+PCM level. The respective energies for
559 SAL are indicated in parentheses. The transition state is indicated with a dashed level.

560

561 Figure 5: The intramolecular H abstraction reaction (**I→II**) and HO_2 dissociation pathway
562 (**II→III**) for TBL and SAL. Energies (kcal/mol) were obtained at the B3LYP/6-
563 31+G(d,p)+PCM level. Transition states and MEP maximum are indicated with dashed levels.

564

565

566

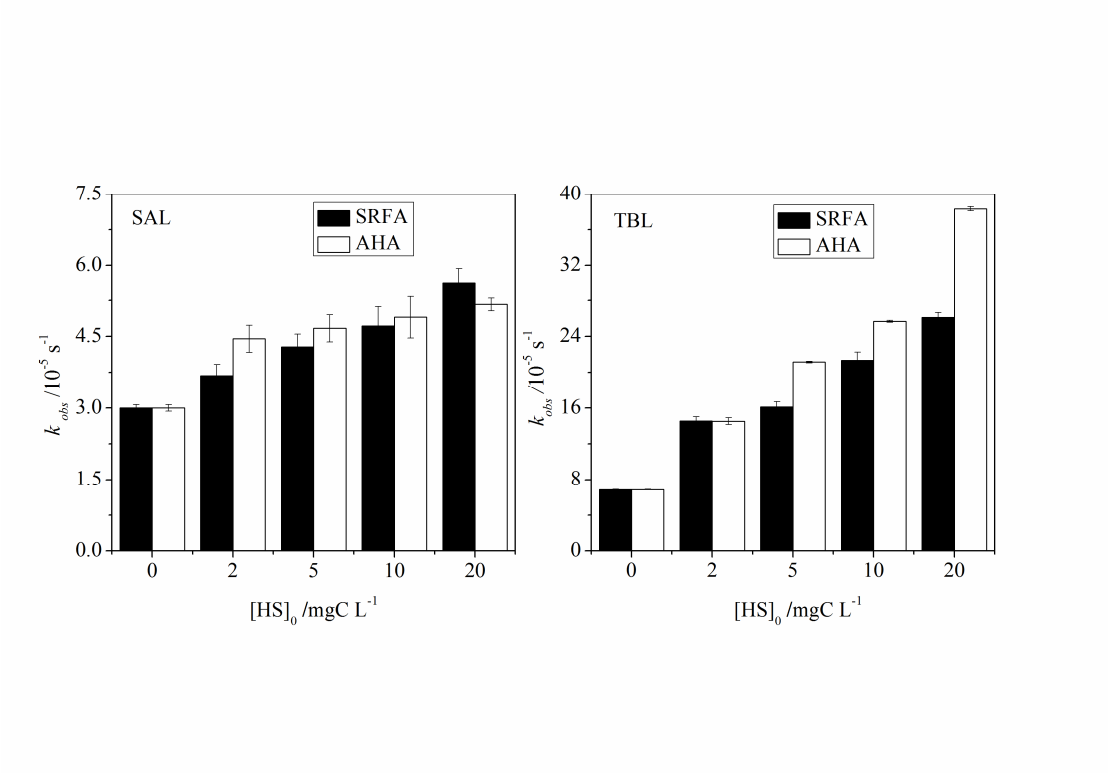

567

568 Figure 1.

569

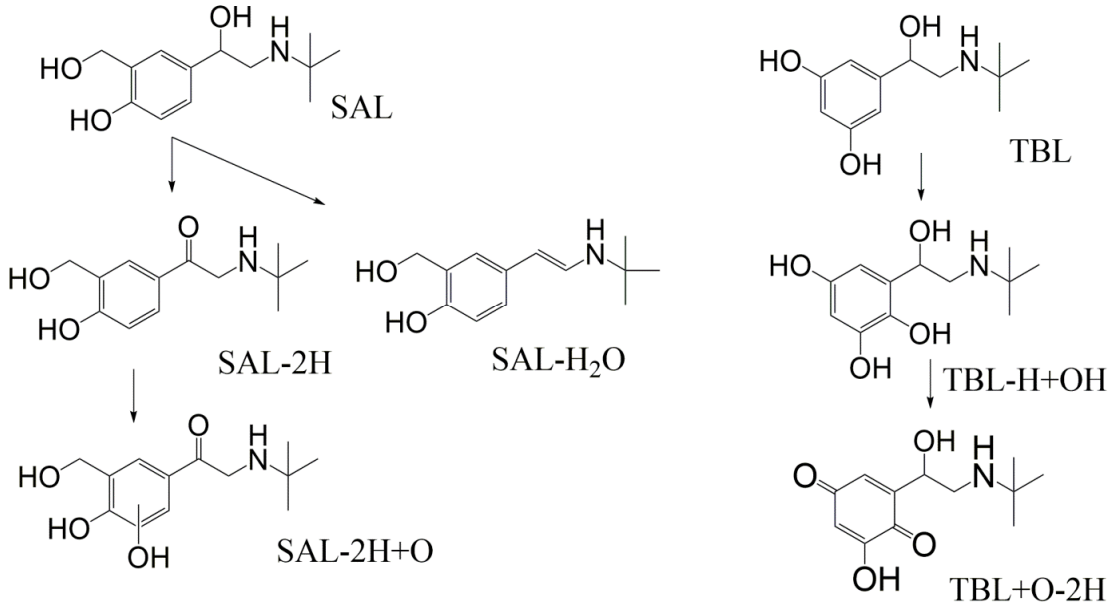

570

571

572

573 Figure 2.

574

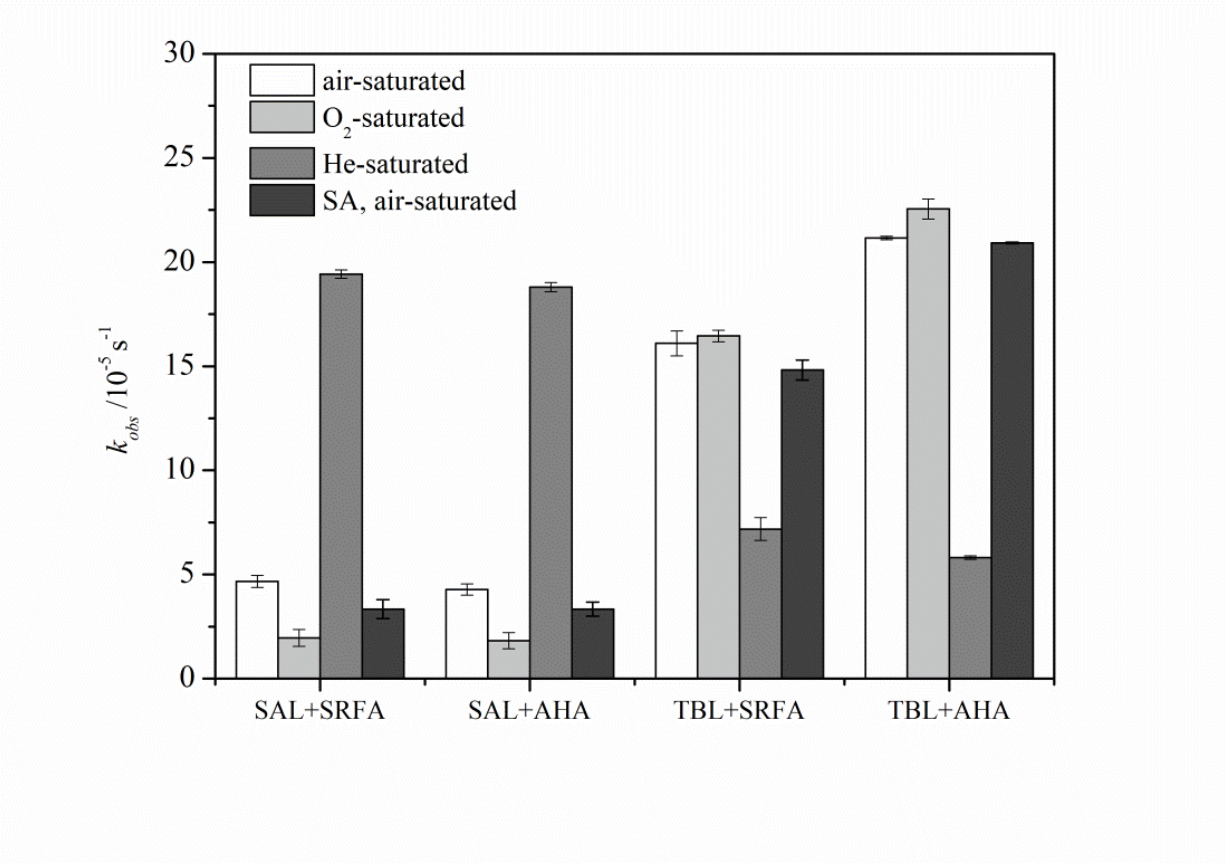

575

576 Figure 3.

577

578

579

580

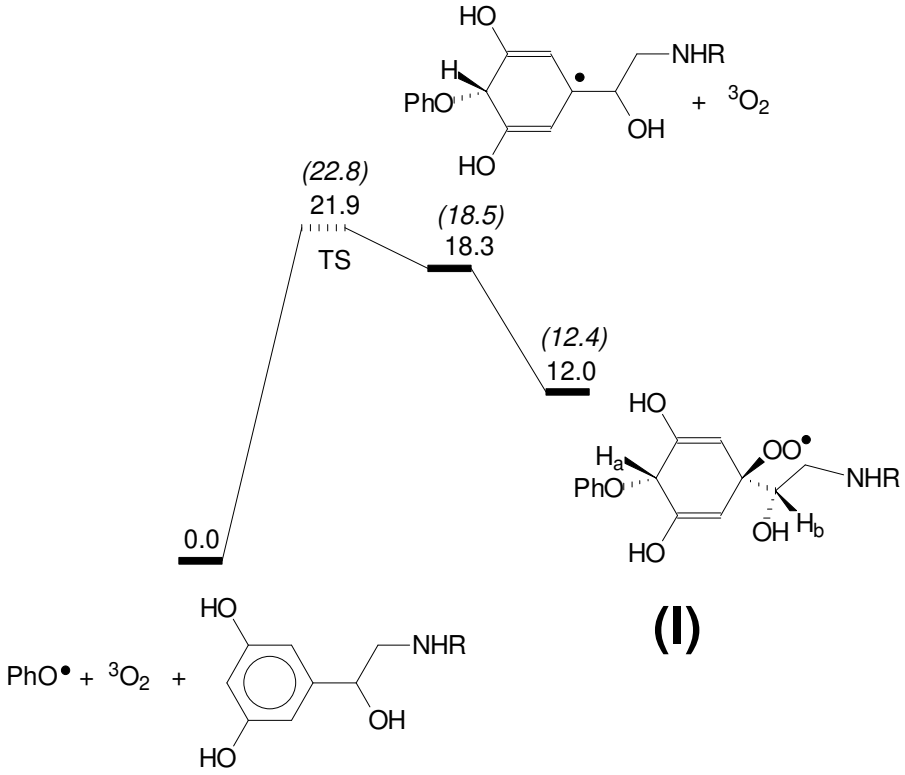

581

582

583 Figure 4

584

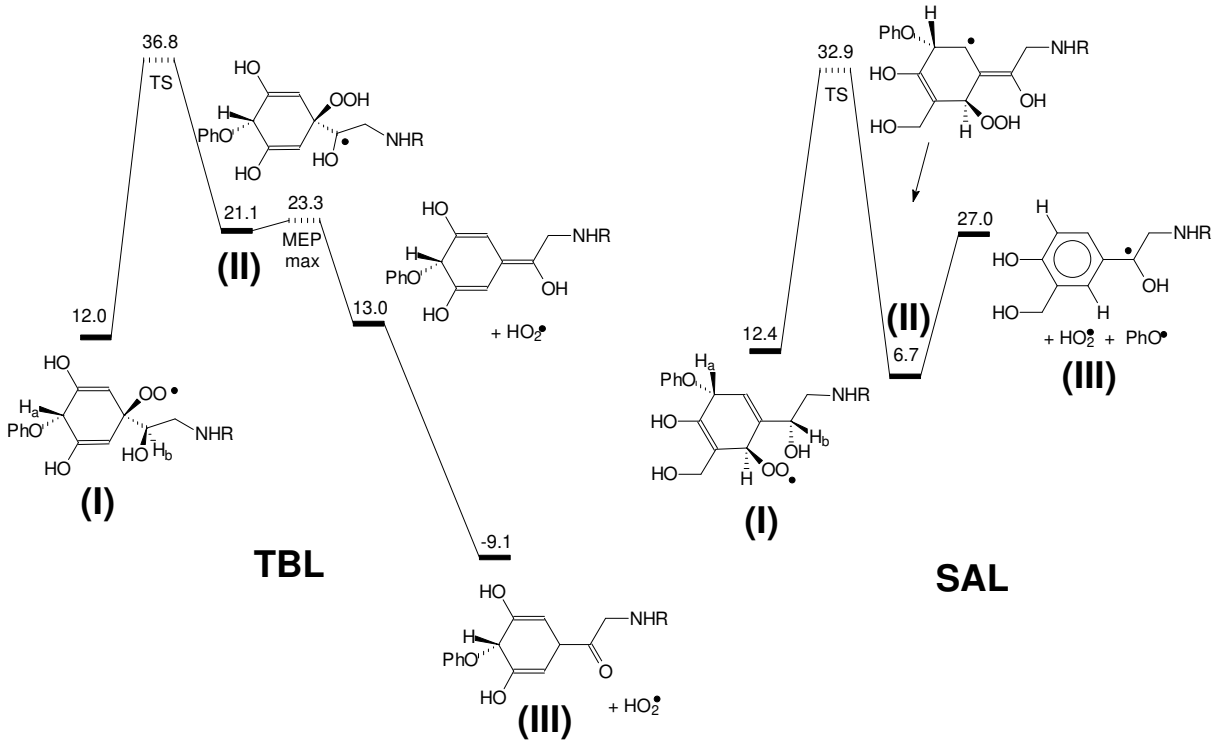

585

586

587

588 Figure 5

589

Conditions	SAL		TBL	
	AHA	SRFA	AHA	SRFA
	$k/10^{-5}$ s^{-1}	$k/10^{-5}$ s^{-1}	$k/10^{-5}$ s^{-1}	$k/10^{-5}$ s^{-1}
corrected k_{direct}	1.2	2.0	2.6	4.2
$k_{indirect}$ under air	3.1	2.8	18.9	12.1
$k_{indirect}$ under He	18.0	17.6	3.3	3.2
$k_{indirect}$ under pure oxygen	0.8	0.2	20.4	12.3

Table 1: Degradation rate constants of SAL and TBL in the presence of SRFA and AHA at 5 mgC L^{-1}. The uncertaincies are of 10%.

603

604

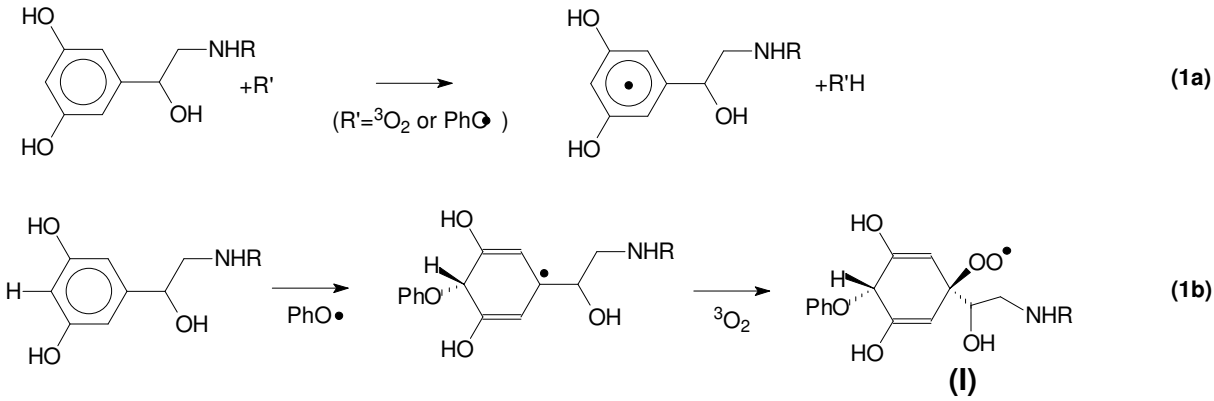

605

606

607 Scheme 1 : Comparison of two initiation reactions that lead to degradation products for TBL.

608 The peroxyl radical in 1b is labeled **I** in the following.

609

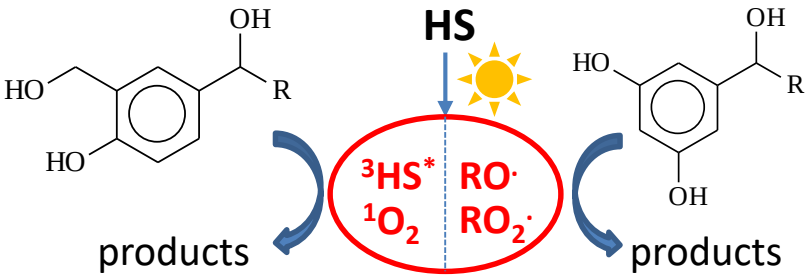
HS
OH
HO
R
HO
OH
HO
R
OH
$^3HS^*$
$^1O_2$
RO·
RO_2·
products
products